

1 **Aerosol properties over the western Mediterranean** 2 **basin: temporal and spatial variability**

3
4 **H. Lyamani^{1,2}, A. Valenzuela^{1,2}, D. Perez-Ramirez^{3,4}, C. Toledano⁵, M. J.**
5 **Granados-Muñoz^{1,2}, F. J. Olmo^{1,2}, and L. Alados-Arboledas^{1,2}**

6 ¹ Andalusian Institute for Earth System Research (IISTA-CEAMA), 18006, Granada,
7 Spain

8 ² Department of Applied Physics, University of Granada, Granada, 18071, Spain

9 ³ Mesoscale Atmospheric Processes Laboratory, NASA Goddard Space Flight Center,
10 20771, Greenbelt-Maryland, USA

11 ⁴ Goddard Earth Sciences Technology and Research, Universities Space Research
12 Association (GESTAR/USRA), Columbia, Maryland, USA

13 ⁵ Atmospheric Optics Group (GOA), University of Valladolid (UVA), 47071
14 Valladolid, Spain

15 Corresponding author: Dr. Hassan Lyamani, (hlyamani@ugr.es)

16 17 **Abstract**

18 This study focuses on the analysis of Aerosol Robotic Network (AERONET) aerosol
19 data obtained over Alborán Island (35.90° N, 3.03° W, 15 m a.s.l) in the western
20 Mediterranean from July 2011 to January 2012. Additional aerosol data from three
21 nearest AERONET stations (Málaga, Oujda and Palma de Mallorca) and the Maritime
22 Aerosol Network (MAN) were also analyzed in order to investigate the aerosol temporal
23 and spatial variations over this scarcely explored region. High aerosol loads over
24 Alborán were mainly associated with desert dust transport from North Africa and
25 occasional advection of anthropogenic fine particles from central European urban-
26 industrial areas. The fine particle load observed over Alborán was surprisingly similar
27 to that obtained over the other three nearest AERONET stations, suggesting
28 homogeneous spatial distribution of fine particle loads over the four studied sites in
29 spite of the large differences in local sources. The results from MAN acquired over the

1 Mediterranean Sea, Black Sea and Atlantic Ocean from July to November 2011
2 revealed a pronounced predominance of fine particles during the cruise period.

3 **1. Introduction**

4 Atmospheric aerosol particles play an important role in the atmosphere because they can
5 affect the Earth's radiation budget directly by the scattering and absorption of solar and
6 terrestrial radiation (e.g., Haywood and Shine, 1997), and indirectly by modifying cloud
7 properties (e.g., Kaufman et al., 2005), and hence have important climate implications.
8 Understanding the influence of atmospheric aerosols on radiative transfer in the
9 atmosphere requires accurate knowledge of their columnar properties, such as the
10 spectral aerosol optical depth, a property related to aerosol amount in atmospheric
11 column (Haywood and Boucher, 2000; Dubovik et al., 2002). Global measurements of
12 columnar aerosol properties including spectral aerosol optical depth can be assessed
13 from satellite platforms (e.g., Kaufman et al., 1997). However, satellite aerosol
14 retrievals suffer from large errors due to uncertainties in surface reflectivity. Currently,
15 the ground sun photometric technique is considered the most accurate one for the
16 retrieval of aerosol properties in the atmospheric column (e.g. Estellés et al., 2012).
17 Thus, many ground based observation networks have been established in order to
18 understand the optical and radiative properties of aerosols and indirectly evaluate their
19 effect on the radiation budget and climate (e.g., AERONET). However, the
20 quantification of aerosol effects is very difficult because of the high spatial and temporal
21 variability of aerosol physical and optical properties (Forster et al., 2007). This high
22 aerosol variability is due to their short atmospheric lifetime, aerosol transformations,
23 aerosol dynamics, different meteorological characteristics, and the wide variety of
24 aerosol sources (Haywood and Boucher, 2000; Dubovik et al., 2002). In this sense,
25 Forster et al. (2007) highlighted the large uncertainties on the aerosol impact on
26 radiation budget. Therefore, monitoring of aerosol properties at different areas in the
27 world can contribute to reduce these uncertainties.

28 Most of the planet is covered by oceans and seas, and thus the study of marine aerosol is
29 a topic of ongoing interest (e.g., Smirnov et al., 2002). Particularly, many efforts are
30 being made to characterize this aerosol type from ground based measurements, leading
31 to the creation of the Maritime Aerosol Network (MAN) as part of the AERONET
32 network (Smirnov et al., 2009). However, MAN lacks of continuous temporal

1 measurements, and thus measurements from remote islands in the oceans and seas are
2 required. Particularly, in the Mediterranean basin aerosol properties are characterized by
3 a great complexity, due to the presence of different types of aerosols such as maritime
4 aerosols from the Mediterranean Sea itself, biomass burning aerosols from forest fires,
5 anthropogenic aerosols transported from European and North African urban areas,
6 mineral dust originated from north African arid areas, and anthropogenic particles
7 emitted from the intense ship traffic in the Mediterranean Sea (e.g., Lelieveld et al.,
8 2002; Barnaba and Gobbi, 2004; Lyamani et al., 2005; Lyamani et al., 2006a, 2006b;
9 Papadimas et al., 2008; Viana et al., 2009; Pandolfi et al., 2011; Alados-Arboledas et
10 al., 2011; Becagli et al., 2012; Valenzuela et al., 2012a, 2012b, Mallet et al., 2013). Past
11 studies revealed that the aerosol load and the aerosol direct radiative effect over the
12 Mediterranean are among the highest in the world, especially in summer (e.g., Lelieveld
13 et al., 2002; Markowicz et al., 2002; Papadimas et al., 2012; Antón et al., 2012).

14 In this framework, the characterization of aerosol over the Mediterranean has received
15 great scientific interest. To date, a large number of studies has been done focusing on
16 the eastern and central regions (e.g., Formenti et al., 1998; Balis et al., 2003;
17 Gerasopoulos et al., 2003; Di Iorio et al., 2003; Kubilay et al., 2003; Pace et al., 2005,
18 2006; Fotiadi et al., 2006; Meloni et al., 2007; Meloni et al., 2008; Di Sarra et al., 2008;
19 Di Biagio et al., 2010; Boselli et al., 2012). However, few studies have been done in the
20 western Mediterranean Basin (Horvath et al., 2002; Alados-Arboledas et al., 2003;
21 Mallet et al., 2003; Estellés et al., 2007; Saha et al., 2008; Pérez-Ramírez et al., 2012,
22 Foyo-Moreno et al., 2014). The majority of these studies have been performed in
23 coastal Mediterranean urban sites largely influenced by local pollution emissions,
24 except those carried out at Crete and Lampedusa islands in the eastern and central
25 Mediterranean Sea regions. In general, columnar aerosol data are scarce over the
26 Mediterranean Sea and almost absent over the western Mediterranean Sea. Thus,
27 measurements of the aerosol properties over the western Mediterranean Sea are needed
28 in order to evaluate the aerosol regimes over this scarcely explored region (Smirnov et
29 al., 2009). In order to fill this gap and provide columnar aerosol properties over the
30 western Mediterranean Sea, the Atmospheric Physics Group of the University of
31 Granada, Spain, in collaboration with Royal Institute and Observatory of the Spanish
32 Navy (ROA), has installed a sun photometer at Alborán, a very small island in the
33 westernmost part of Mediterranean Sea located midway between the African and

1 European continents. Currently, this station is part of AERONET network
2 (<http://aeronet.gsfc.nasa.gov>).

3 This study focuses on the characterization of aerosol load and aerosol types as well as
4 on their temporal variability over Alborán Island in the western Mediterranean from 1
5 July 2011 to 23 January 2012. In addition, special attention is given to the conditions
6 responsible for large aerosol loads over this Island and much attention is paid to identify
7 the potential aerosol sources affecting Alborán. Furthermore, additional aerosol
8 properties from three AERONET stations (Málaga, Oujda and Palma de Mallorca)
9 surrounding Alborán Island and from a MAN cruise over the Mediterranean Sea, Black
10 Sea and Atlantic Ocean (Figure 1) are analyzed here to investigate the spatial aerosol
11 variation over the Mediterranean basin.

12 The work is structured as follows. In section 2 we describe the instrumentation used and
13 the experimental sites. Section 3 is devoted to the main results, where we analyze the
14 aerosol optical properties at Alborán Island and the spatial variability of aerosol
15 properties in the Mediterranean. Finally, in section 4 we present the summary and
16 conclusions.

17 **2. Instrumentation and study sites**

18 **2.1. AERONET measurements.**

19 Columnar aerosol properties were measured by a CIMEL CE-318-4 sun photometer,
20 which is the standard automated sun photometer used in the AERONET network
21 (Holben et al., 1998). This instrument has a full view angle of 1.2° and makes direct sun
22 measurements at 340, 380, 440, 500, 670, 870, 940 and 1020 nm (nominal
23 wavelengths). The direct sun measurements are then used to retrieve the aerosol optical
24 depth at each wavelength, $\delta_a(\lambda)$, except for 940 nm which is used to compute
25 precipitable water vapor (Holben et al., 1998). Detailed information about the CIMEL
26 sun photometer can be found in (Holben et al., 1998). The total estimated uncertainty in
27 $\delta_a(\lambda)$ provided by AERONET is of ± 0.01 for $\lambda > 440$ nm and ± 0.02 for shorter
28 wavelengths (Holben et al., 1998). Furthermore the spectral dependency of the $\delta_a(\lambda)$ has
29 been considered through the Ångström exponent, $\alpha(440-870)$, calculated in the range
30 440–870 nm. The Ångström exponent provides an indication of the particle size (e.g.,
31 Dubovik et al., 2002). Small values of the Ångström coefficient ($\alpha(440-870) < 0.5$)

1 suggest a predominance of coarse particles, such as sea salt or dust, while
2 $\alpha(440-870) > 1.5$ indicates a predominance of small particles such as sulphate, nitrate
3 and biomass burning particles. Also included in the analysis are aerosol optical depths
4 at 500 nm for fine mode ($\delta_F(500 \text{ nm})$) and for coarse mode ($\delta_C(500 \text{ nm})$) as well as the
5 fine mode fraction (FMF) (ratio of $\delta_F(500 \text{ nm})$ to $\delta_a(500 \text{ nm})$), determined using the
6 spectral de-convolution algorithm method developed by O'Neill et al. (2003). In this
7 study, the level 2 AERONET aerosol data are used.

8 **2.2 AERONET stations**

9 This study focuses on the AERONET sun photometer measurements acquired at the
10 Alborán Island (35.90° N, 3.03° W, 15 m a.s.l), in the western Mediterranean Sea, from
11 1 July 2011 to 23 January 2012. Alborán is a small island with an approximate surface
12 of 7 hectares, located ~ 50 km north of the Moroccan coast and 90 km south of the
13 Spanish coast (Fig. 1). Currently, only 12 members of a small Spanish Army garrison
14 live on the island. The island and its surrounding area are declared a natural park and
15 marine reserve. There is no significant local anthropogenic emission source at Alborán;
16 however, the island is just south of an important shipping route
17 (www.marinetraffic.com). Due to its location, Alborán Island is expected to be affected,
18 depending on regional circulation, by anthropogenic pollutants originated in urban and
19 industrial European areas, anthropogenic particles emitted from the ship traffic, desert
20 dust transported from North African arid regions and maritime aerosols from the
21 Mediterranean Sea. The climate of the region depends strongly on the Azores
22 anticyclone. Winter is mainly characterized by low pressure systems passing over the
23 Iberian Peninsula, resulting in the prevalence of westerly winds and enhanced rainfall.
24 In this season, the weather is unstable, wet and windy. In summer, the well-established
25 Azores high pressure produces dry and mild weather with easterly winds that combine
26 with sea/land breezes created by the aridity of the coastal mountains (Sumner et al.,
27 2001).

28 In addition, to investigate the spatial variation of aerosol properties over the western
29 Mediterranean, we used AERONET data obtained from 1 July 2011 to 23 January 2012
30 over three AERONET stations surrounding Alborán Island; Oujda, Málaga and Palma
31 de Mallorca (see Fig. 1). These sites cover different environments including, urban,
32 coastal and island sites, respectively, and have different background aerosol

1 characteristics. Palma de Mallorca (39.35° N, 2.39° E, 13 m a.s.l), the capital of the
2 Balearic Islands, is the largest city in the Mallorca Island with a population of around
3 400,000. It is located in the western Mediterranean Sea, about 250 km from the African
4 continent and 190 km from the Spanish coast. Málaga (36.72°N, 4.5°W, 40 m a.s.l),
5 with a population of around 600,000 is the major coastal city in southeast Spain on the
6 Mediterranean coast. Oujda city (34.65° N, 1.89° W, 450 m a.g.l) is located in eastern
7 Morocco, 60 km south of the Mediterranean Sea, with an estimated population of
8 450,000.

9 **2.3. Maritime Aerosol Network measurements**

10 Furthermore, we used ship borne sun photometer measurements collected on-board the
11 Nautilus_11 on the Mediterranean Sea, Atlantic Ocean and Black Sea during the period
12 26 July - 13 November 2011. These measurements were made in the framework of the
13 Maritime Aerosol Network (MAN), a component of AERONET (Smirnov et al., 2011).
14 More detailed information about the Nautilus_11 cruise track can be found in
15 (http://aeronet.gsfc.nasa.gov/new_web/cruises_new/Nautilus_11.html). MAN uses
16 Microtops II hand held sun photometers and utilizes calibrations and data processing
17 procedures of AERONET network. The Microtops II sun photometer used in this cruise
18 acquires direct sun measurements at 440, 500, 675 and 870 nm. The estimated
19 uncertainty of the optical depth in each channel is around ± 0.02 (Knobelspiese et al.,
20 2004). Level 2 MAN data are used in this study.

21 **2.4. Air mass trajectories**

22 To characterize the transport pathways and the origins of air masses arriving at our
23 studied AERONET sites, 5-day backward trajectories ending at 12:00 UTC at these
24 sites for 500, 1500, 2500, 3500, 4500 and 5000 m above ground level were calculated
25 using the HYSPLIT model for days with AERONET measurements (Draxler and
26 Rolph, 2003). In addition, backward trajectories ending at the different points of MAN
27 cruise for 500, 1500, 2500, 3500, 4500 and 5000 m above ground level were also
28 performed for days with MAN observations. The HYSPLIT model version employed
29 uses GDAS meteorological data and includes vertical wind.

1 3. Results and discussion

2 3.1. Temporal evolution of aerosol properties over Alborán Island

3 Fig. 2 shows the temporal evolutions of daily mean values of aerosol optical depths at
4 500 and 1020 nm and $\alpha(440-870)$ measured at Alborán Island in the western
5 Mediterranean from 1 July 2011 to 23 January 2012. There are some gaps in $\delta_a(\lambda)$ and
6 $\alpha(440-870)$ data series due to some technical problems and the presence of clouds
7 (invalid data). Table 1 presents a statistical summary of daily average values of all the
8 analysed aerosol properties. One of the main features observed is the large variability of
9 $\delta_a(\lambda)$ (for example, $\delta_a(500\text{ nm})$ ranged from 0.03 to 0.54) that is primarily related to
10 changes in the air masses affecting the study area, as can be seen hereafter. The
11 coefficient of variation (COV), defined as the standard deviation divided by the mean
12 value, can be used to compare the variability of different data sets. As shown in Table 1,
13 the $\delta_a(\lambda)$ at 1020 nm (with COV of 91%) showed much greater variability than at 340
14 nm (with COV of 60%). It is well known that $\delta_a(\lambda)$ at higher wavelengths is more
15 affected by naturally produced coarse particles (radius above 0.5 μm) like dust and sea
16 salt particles, while $\delta_a(\lambda)$ at smaller wavelengths is more sensitive to the fine particles
17 (radius below 0.5 μm) such as those from anthropogenic activities or biomass-burning.
18 Thus, the higher variability of $\delta_a(\lambda)$ for larger wavelengths indicates strong variability in
19 the coarse particle load (dust or sea salt) over Alborán Island. This result is also
20 supported by the larger COV of $\delta_c(500\text{ nm})$ as compared to $\delta_f(500\text{ nm})$ (Table 1).
21 Aerosol salt emission variations due to the wind speed variation and the changes in the
22 frequency and intensity of dust intrusions over the Island may explain the large
23 variability in the coarse particle component and hence the large $\delta_a(\lambda)$ variability for
24 large wavelengths. Moreover, coarse particles have shorter residence time in the
25 atmosphere in comparison with fine particles, which could explain also the large $\delta_c(\lambda)$
26 variability. On the other hand, $\alpha(440-870)$ values also show large variability and vary
27 from 0.2 to 1.7 with mean value of 0.8 ± 0.5 , indicating different atmospheric conditions
28 dominated by different aerosol types (coarse particles, fine aerosols and/or different
29 mixtures of both coarse and fine particles). It is noted that on 70% of the analysed days
30 the values of $\alpha(400-870)$ were lower than 1, suggesting that coarse particles dominated
31 the aerosol population over the Alborán Island for most of the analysed days. This is
32 further supported by the analysis of fine mode fraction which ranged from 0.20 to 0.90

1 (mean value of 0.47 ± 0.15); with daily mean values less than 0.5 on 65% of the analysed
2 days.

3 The observed mean $\delta_a(500 \text{ nm})$ value over Alborán Island was significantly higher (by
4 factor of 2) than that reported by Smirnov et al. (2002) ($\delta_a(500 \text{ nm})$ in the range 0.06-
5 0.08) for open oceanic areas in the absence of long-range transport influences.
6 Moreover, the mean $\delta_a(500 \text{ nm})$ and $\alpha(440-870)$ values obtained in this study were
7 larger than the global mean $\delta_a(500 \text{ nm})$ value of 0.11 and $\alpha(440-870)$ of 0.6 reported for
8 maritime aerosols by Smirnov et al. (2009). On other hand, average aerosol optical
9 depths at 495.7 nm of 0.24 ± 0.14 and $\alpha(415-868)$ of 0.86 ± 0.63 were obtained from multi
10 filter rotating shadowband radiometer at Lampedusa Island (in the central
11 Mediterranean Sea) during July 2001-September 2003 (Pace et al., 2006). Using
12 AERONET data measured in Crete Island (eastern Mediterranean Sea) during 2003-
13 2004, Fotiadi et al. (2006) reported mean $\delta_a(500 \text{ nm})$ value of 0.21 and $\alpha(440-870)$ of
14 1.1. The differences between aerosol properties observed over Alborán, Lampedusa and
15 Crete Islands could be explained in terms of differences in the period and duration of
16 the measurements, in air mass circulation and in the methodologies employed. Later we
17 compare the results obtained over Alborán to those observed over three nearby
18 AERONET stations (during the same period and using the same type of instruments).

19 According to the Smirnov et al. (2003) criterion, pure maritime situations can be
20 generally found when $\delta_a(500 \text{ nm}) < 0.15$ and $\alpha(440-870)$ is less than 1. Considering this
21 criterion, pure maritime situations were observed over Alborán Island on 40% of the
22 analyzed days. According to back trajectory analysis, almost all these days were
23 characterized by advection of clean Atlantic air masses over the study area. In addition,
24 the majority of these pure maritime cases were observed during the wet season from
25 November to January. This result is in agreement with the study performed at the Island
26 of Lampedusa, in the central Mediterranean, showing that pure maritime situations are
27 usually observed during Atlantic air advection (Pace et al., 2006). However, clean
28 maritime conditions observed over Alborán Island during the analyzed period are more
29 frequent than those observed over Lampedusa. Pace et al. (2006) showed that clean
30 maritime conditions are rather rare over the central Mediterranean due to the large
31 impact of natural and anthropogenic sources. The difference in the occurrences of clean
32 maritime conditions at these two sites can be explained by their different locations.
33 Alborán is closer to the Atlantic Ocean than is Lampedusa, and the Atlantic air masses

1 reaching Lampedusa may be more influenced by anthropogenic aerosol during their
2 passage over Mediterranean Sea and continents.

3 Threshold values for $\delta_a(500 \text{ nm})$ and $\alpha(440-870)$ have been widely used in remote
4 sensing to identify marine aerosol type. For example, Smirnov et al. (2003) used $\delta_a(500$
5 $\text{ nm}) \leq 0.15$ and $\alpha(440-870) \leq 1$ and Sayer et al. (2012a,b) proposed $\delta_a(500 \text{ nm}) \leq 0.2$
6 and $0.2 \leq \alpha(440-870) \leq 1$ while Toledano et al. (2007) used $\delta_a(500 \text{ nm}) \leq 0.15$ and
7 $\alpha(440-870) \leq 0.6$ for identifying pure maritime situations. However, the proposed
8 threshold values for $\delta_a(500 \text{ nm})$ and $\alpha(440-870)$ to identify maritime aerosol type are
9 purely empirical. Therefore, not all observations that meet these thresholds will
10 represent the pure maritime aerosol. In fact, in Alboran Island we found measurements
11 that fulfill these criteria but that are not associated with pure maritime conditions. In this
12 sense, in Fig. 3 we show the $\delta_a(500 \text{ nm})$ and $\alpha(440-870)$ observed on 26 August, 2011.
13 During this day, the $\delta_a(500 \text{ nm})$ values ranged from 0.06 to 0.13 with mean daily value
14 of 0.09 ± 0.01 and $\alpha(440-870)$ was in the range 0.3-0.6, indicating clean atmospheric
15 condition dominated by coarse particles. Thus, according to the above criteria this day is
16 classified as pure maritime case. However, the back trajectory analysis and MSG
17 satellite image (Thieuleux et al., 2005) for August 26 revealed the presence of dust over
18 Alborán Island (Figure 3). Therefore, care must be taken when using $\delta_a(500 \text{ nm})$ and
19 $\alpha(440-870)$ thresholds for discriminating the pure maritime cases since dusty situations
20 with low dust loads can be confused with pure maritime conditions. Additional
21 information such as air mass back trajectory or satellite images is needed for better
22 identifying the pure maritime cases.

23 As can be seen in Fig. 2, there were several days strongly influenced by aerosols, with
24 $\delta_a(500 \text{ nm})$ values exceeding 0.3. High aerosol loads ($\delta_a(500 \text{ nm}) > 0.3$) over Alborán
25 Island were observed on 30 of the 160 analysed days. All these events were observed
26 from July to October. In 27 of these cases, the mean daily $\alpha(440-870)$ values were
27 lower than 0.8 and FMF lower than 0.5; suggesting predominance of coarse particles as
28 either sea salt or dust transported from desert areas. According to the analyses of back
29 trajectories and MODIS satellite images (not shown), all these 27 cases were related to
30 dust intrusions from North Africa. It is important to note that in these dust events, the
31 $\delta_F(500 \text{ nm})$ values were also relatively high (for this remote site) and ranged from 0.07
32 to 0.20 with mean value of 0.12 ± 0.03 . These results highlight a considerable
33 contribution of fine mode particles (either dust or anthropogenic or both) to the aerosol

1 population (FMF ranged from 20% to 52%) during these dust events. Back trajectory
2 analysis for dusty days with highest fine aerosol load revealed that the air masses
3 reaching the study area at low levels (at 500 m or 1500 m level) have originated over
4 Europe and the Mediterranean Sea. However, during desert dust events with lowest fine
5 aerosol loads, none of the air masses affecting the study area come from Europe or
6 Mediterranean Sea, which points out significant contribution of anthropogenic particles
7 to the fine mode fraction of $\delta_a(500 \text{ nm})$ during desert dust events associated with large
8 loads of fine aerosol particles.

9 The remaining high aerosol load events were observed from 30 September to 4 October
10 2011 (Fig. 4). During these days the high aerosol loads were associated with relatively
11 high $\alpha(440-870)$ values that reached the highest $\alpha(440-870)$ value (about 1.6) during
12 the entire study on 4 October. During these days, the $\delta_F(500 \text{ nm})$ values were also high
13 (>0.19) and reached the highest mean daily value of 0.33 on 4 October. This behavior
14 suggests a predominance of fine particles transported from continental industrial/urban
15 areas as there is no local anthropogenic activity in Alborán. The high $\delta_a(\lambda)$ values
16 observed in this event were associated with persistent intense high pressure systems
17 centered over the Azores, which favor transport of anthropogenic particles emitted in
18 Europe to Alborán Island. **Indeed, on this day the air mass ending at 1500 m a.g.l (Fig.**
19 **4c) came from central Europe and traveled at low altitude on the last 3 days before its**
20 **arrival at Alborán Island, over an area with a great sulfate surface concentration**
21 **according to NAAPS model (Fig. 4d,f).** Therefore, these air masses might pick up fine
22 anthropogenic particles in their way to Alborán Island, which may explain the high
23 values of both $\delta_a(500 \text{ nm})$ and $\alpha(440-870)$ parameters observed during this event. Thus,
24 the desert dust transport appears to be a main cause of high aerosol loads while transport
25 from central European urban areas is associated with occasional large aerosol loads over
26 Alboran Island. These results are in accordance with those reported by Fotiadi et al.
27 (2006) for Crete, who found the highest values of $\delta_a(\lambda)$ primarily during southeasterly
28 winds, associated with coarse dust aerosols, and to a lesser extent to northwesterly
29 winds associated with fine aerosols originated in urban industrial European areas.

30 **3.2. Monthly variation of aerosol properties over Alborán Island**

31 Fig. 5 shows the monthly mean values of $\delta_a(500 \text{ nm})$, $\delta_F(500 \text{ nm})$ and $\delta_C(500 \text{ nm})$ as
32 well as $\alpha(440-870)$ and FMF with the corresponding standard deviations for the

1 analysed period. The monthly average data are calculated from daily averaged data. The
2 largest values of $\delta_a(500 \text{ nm})$, reflecting high aerosol load, were observed during July-
3 October while the lowest values (0.06-0.08) were measured from November to January
4 (Fig. 5a). On other hand, the monthly mean values of $\alpha(440-870)$ and FMF were lower
5 than 1.0 and 0.5 respectively, indicating a relatively high abundance of coarse particles
6 in each month of the analysed period, except in October (Fig. 5b). For October, the
7 mean $\alpha(440-870)$ was 1.1 ± 0.4 and the FMF 0.63 ± 0.20 , indicating an increase in fine
8 particle contribution during this month (Fig. 5b). It is also worth noting that both $\delta_F(500$
9 $\text{ nm})$ and $\delta_C(500 \text{ nm})$ showed a pronounced increase during July-October, suggesting
10 increased loads of both fine and coarse particles during these months (Fig. 5a).
11 Moreover, $\delta_C(500 \text{ nm})$ reached its maximum in August while $\delta_F(500 \text{ nm})$ peaked in
12 October (Fig. 5a).

13 This pronounced change in aerosol loads from summer to winter in 2011 is primarily
14 due to the seasonal change in atmospheric circulation over the Mediterranean (Fig. 5c).
15 The increased coarse aerosol load observed during July-October was associated with the
16 high frequency of desert dust intrusions in summer in comparison to November-January
17 (Fig. 5c). In fact, 40%, 70 %, 41% and 14% of measurement days in July, August,
18 September and October were associated with Saharan dust intrusions while in
19 November-January there was no Saharan dust intrusion (Fig. 5c). Moreover, the air
20 mass recirculation over the western Mediterranean especially in summer (Millan et al.,
21 1997) along with the increased photochemical activity due to the high insolation during
22 this season may favor the accumulation of fine aerosols that can explain the high fine
23 particle loads during July-October in comparison with November-January. In addition,
24 the presence of these fine aerosol particles may be favored by pollution transport from
25 Europe and coastal urban industrial areas in northeast Africa. In this sense, the highest
26 fine mode aerosol optical depth observed in October was associated with the increase in
27 the frequency of air masses coming from European urban areas (see for example Fig. 4).
28 The low aerosol loads registered in November-January can be explained by the high
29 frequency of clean Atlantic air advection (70-100%) and the absence of Saharan dust
30 intrusions (Fig. 5c) as well as efficient wet removal aerosol processes due to cloudy
31 conditions and precipitation in this period. These results highlight the important role of
32 the large scale circulation on monthly aerosol variation over Alborán Island.

1 **3.3. Spatial variability of aerosol properties over western Mediterranean** 2 **region**

3 AERONET data of level 2 from Alborán and three AERONET stations surrounding the
4 Island (see Fig. 1) obtained from 1 July 2011 to 23 January 2012 are considered in this
5 study to investigate the spatial variation of aerosol optical properties over the western
6 Mediterranean region. For analyzing the spatial aerosol variability we compared the
7 aerosol data obtained over Alborán during 1 July 2011 - 23 January 2012 with those
8 observed over these nearby sites using only time coincident measurements.

9 Temporal evolutions of daily mean values of $\delta_a(500 \text{ nm})$ from 1 July 2011 to 23 January
10 2012 obtained over Alborán Island and Málaga stations are shown in Fig. 6a. Daily
11 mean data were calculated only from time coincident measurements for direct
12 comparison. Málaga is located approximately 150 km northwest of Alborán. The
13 temporal variations of daily mean values of $\delta_a(500 \text{ nm})$ were similar for both sites on
14 most days of the analyzed period, indicating similarities in the processes that control the
15 aerosol load over both sites. In fact, high correlation in $\delta_a(500 \text{ nm})$ with correlation
16 coefficient, R , of 0.75 between these two sites was found. Similar results were obtained
17 when comparing $\delta_a(500 \text{ nm})$ over Alborán with those in Oujda ($R=0.8$) and Palma de
18 Mallorca ($R=0.6$), Fig. 6b,c. However, large differences are also present on some days
19 (e.g. on August 8th 2011 at Alboran Island we registered $\delta_a(500 \text{ nm})$ above 0.5 while at
20 Málaga the values were below 0.1). These differences are due, in large part, to the
21 differences in the times of occurrence and intensity of Saharan dust intrusions over
22 these sites. In fact, the correlation in $\delta_F(500 \text{ nm})$ between Alborán Island and Málaga,
23 $R=0.86$, was higher than the correlation in $\delta_C(500 \text{ nm})$, $R=0.65$. Similar results were
24 obtained when comparing the aerosol properties over Alborán with those in Oujda
25 ($R=0.82$ for $\delta_F(500 \text{ nm})$ and $R=0.70$ for $\delta_C(500 \text{ nm})$) and Palma de Mallorca ($R=0.67$
26 for $\delta_F(500 \text{ nm})$ and $R=0.32$ for $\delta_C(500 \text{ nm})$).

27 Table 2 shows average values of $\delta_a(\lambda)$, $\alpha(440-870)$, $\delta_F(500 \text{ nm})$ and FMF as well as the
28 number of measurement days for each comparison (Alborán-Málaga, Alborán-Oujda
29 and Alborán-Palma de Mallorca). Only days with coincident measurements obtained at
30 Alborán and at each one of the additional AERONET stations from 1 July 2011 to 23
31 January 2012 were used for direct comparisons. For $\lambda > 500 \text{ nm}$, values of $\delta_a(\lambda)$ were
32 slightly larger over Alborán than over Málaga (Table 2). Indeed, the mean $\delta_a(1020 \text{ nm})$

1 value obtained at Alborán was 35% larger than that observed over Málaga. This
2 indicates that the coarse particles levels were significantly larger over Alborán in
3 comparison with Málaga during the analysed period. In fact, the mean $\delta_C(500 \text{ nm})$ for
4 the entire analysed period was slightly higher (0.09 ± 0.08) at Alborán in comparison
5 with Málaga (0.06 ± 0.05). The lower coarse particles load over Málaga as compared to
6 Alborán is likely due to the higher frequency of Saharan dust outbreaks over Alborán as
7 compared to Málaga and also to dust deposition in its way from Alborán to Málaga. On
8 other hand, for $\lambda < 500 \text{ nm}$, the mean value of $\delta_a(\lambda)$ over Alborán was almost similar to
9 that over Málaga (Table 2). It is interesting to note that the mean $\delta_F(500 \text{ nm})$ value for
10 the entire studied period observed over Alborán (0.09 ± 0.06) was similar to that obtained
11 (0.09 ± 0.06) over the Málaga urban coastal site, suggesting similar concentrations of fine
12 particles over both sites. This result is quite surprising because Málaga is a coastal city
13 with significant local anthropogenic emissions in comparison to Alborán where there
14 are no local anthropogenic activities. As we commented before, Alborán Island is
15 located near an important shipping route and hence it is expected to be highly
16 influenced by ship emissions. Thus, these results suggest that emissions from ships
17 and/or from urban-industrial areas in Mediterranean countries could play in Alborán a
18 similar role to that played by anthropogenic particles in Málaga. Further studies using
19 chemical analysis of particles sampled in-situ are needed to evaluate this hypothesis.

20 The comparison of the aerosol properties obtained at Oujda and Alborán Island is also
21 shown in Table 2. In this case, the $\delta_a(\lambda)$ at all wavelengths were lower at Alborán than
22 at Oujda, indicating lower aerosol concentrations over Alborán. However, $\delta_F(500 \text{ nm})$
23 was similar over Oujda and Alborán (Table 2), indicating similar fine particle loading
24 over both sites. This result is again surprising because Oujda is an urban site with
25 significant local anthropogenic emissions in comparison to Alborán Island where there
26 is no local anthropogenic activities. These results also point to the significant role that
27 anthropogenic emissions from traffic ships and/or Mediterranean countries may play
28 over Alborán. On the other hand, $\delta_C(500 \text{ nm})$ obtained over Oujda (0.14 ± 0.15) was
29 higher than that observed over Alborán (0.11 ± 0.10), indicating higher coarse particle
30 concentrations over Oujda. The large coarse particle load over Oujda may result from its
31 proximity to dust sources and local dust re-suspension.

32 The mean $\delta_a(\lambda)$ values at all wavelengths over Alborán were higher than those observed
33 over Mallorca, especially at the larger wavelengths which are more influenced by coarse

1 particles (Table 2). However, as in the other cases, $\delta_F(500 \text{ nm})$ was very similar over
2 both sites (Table 2) in spite of the large distance (about 650 km) separating the sites and
3 site characteristic differences. These results suggest homogeneous spatial distribution of
4 fine particle loads over the four studied sites in spite of the large differences in local
5 sources. On the other hand, the observed decrease in $\delta_a(500 \text{ nm})$ from south (Alborán)
6 to north (Mallorca) may be attributed to the proximity of Alborán Island to the dust
7 sources in north Africa as compared to Mallorca. A gradient in dust load from south to
8 north in western Mediterranean has also been reported by other authors (e.g., Moulin et
9 al., 1998; Barnaba and Gobbi, 2004). Overall, based on the above comparisons it may
10 be concluded that $\delta_C(\lambda)$ showed a south-to-north decrease in this region of western
11 Mediterranean, while the fine mode aerosol optical depth was fairly similar over these
12 sites.

13 **3.4. Variability of aerosol properties during a MAN cruise**

14 From 26 July to 13 November 2011 the Maritime Aerosol Network acquired
15 measurements over the whole Mediterranean Sea, Black Sea and Atlantic Ocean from
16 the ship Nautilus_11. Fig. 7 shows $\delta_a(500 \text{ nm})$, $\delta_F(500 \text{ nm})$, $\delta_C(500 \text{ nm})$ and FMF
17 obtained during this cruise. The measurements made over the Mediterranean Sea were
18 divided, on the basis of the differences in the aerosol sources and air masses affecting
19 each area, into three regions, western, central and eastern Mediterranean. As can be seen
20 from Fig. 7, all the analysed aerosol properties showed large variability with no evident
21 pattern during the cruise period. This large variability in aerosol properties during this
22 cruise can be explained by the different aerosol sources and air masses that affected
23 each region during the measurement period (see below). For the entire cruise period, the
24 $\delta_a(500 \text{ nm})$ varied from 0.08 to 0.70 with a mean value of 0.22 ± 0.12 . On the other hand,
25 $\delta_F(500 \text{ nm})$ also showed large variability and ranged between 0.04 and 0.60 with a mean
26 value of 0.16 ± 0.10 while $\delta_C(500 \text{ nm})$ fluctuated within the range 0.01-0.30 with mean
27 value of 0.06 ± 0.04 . For 85% of the measurements, the fine mode fraction was in the
28 range 0.52-0.96, indicating the predominance of situations dominated by fine mode
29 particles during this cruise.

30 The highest $\delta_a(500 \text{ nm})$ values ranging from 0.20 to 0.46 with a mean value of
31 0.35 ± 0.09 were observed over the western Mediterranean Sea during the cruise period
32 28 September-08 October (Table 3). Also, $\delta_F(500 \text{ nm})$ values were highest (varying in

1 the range of 0.14-0.40 with a mean value of 0.29 ± 0.09) over the western Mediterranean.
2 These high aerosol loads were associated with high FMF values in the range 0.70-0.87,
3 which show the predominance of fine anthropogenic particles over this area during this
4 period (Fig. 7b). According to the back trajectory analyses, the air masses that affected
5 the western Mediterranean region during this period come from European urban-
6 industrial areas which explains the observed large values of $\delta_a(500\text{ nm})$ and the
7 predominance of fine mode particles (see for example Fig. 4c). The aerosol loads were
8 also relatively high over the Black Sea ($\delta_a(500\text{ nm})$), ranging from 0.08 to 0.68 with a
9 mean value of 0.25 ± 0.16 during 26 July-15 August cruise period) and were strongly
10 dominated by fine particles as showed by FMF values ranging from 0.64 to 0.94. The
11 large values of $\delta_a(500\text{ nm})$ and those of $\delta_F(500\text{ nm})$ ($\delta_F(500\text{ nm})$ in the range 0.07-0.60)
12 and the predominance of the fine mode over the Black Sea during this cruise period was
13 associated, according to the HYSPLIT back trajectory analyses, with air masses coming
14 from north-eastern Europe (Figure not shown); this region has been identified as a
15 strong source of pollutants and biomass burning particles during summer (e.g., Barnaba
16 and Gobbi, 2004). In contrast, the lowest $\delta_a(500\text{ nm})$ values (varying in the range 0.08-
17 0.26 with mean value of 0.14 ± 0.06) were observed over eastern Mediterranean at the
18 end of the cruise (5-13 November). These low $\delta_a(500\text{ nm})$ values were associated with
19 FMF ranging between 0.30 and 0.64, showing a predominance of coarse aerosol over
20 this area during this period. It is worth noting that the aerosol loads over the eastern
21 Mediterranean during 5-13 November decreased drastically in comparison with the
22 aerosol levels observed in the same region during the cruise period from 18 August to
23 13 September (Table 3). The decrease was more pronounced for the fine particle load;
24 $\delta_F(500\text{ nm})$ decreased from 0.16 ± 0.07 in the first measurements over eastern
25 Mediterranean to 0.07 ± 0.02 in the last ones. In contrast, $\delta_C(500\text{ nm})$ showed an increase
26 from 0.04 ± 0.02 during 18 August-12 September to 0.08 ± 0.04 during 5-13 November.
27 This drastic change may be explained by the seasonal changes in the meteorological
28 conditions. In this sense, the last measurements over the eastern Mediterranean Sea
29 were obtained during the end of autumn when aerosol wet deposition is more effective
30 and secondary aerosol formation is less important than in summer, which may explain
31 the lower aerosol loads observed at the end of the expedition.

4. Conclusions

AERONET sun photometer measurements obtained over Alborán Island and three adjacent sites in the western Mediterranean were analyzed in order to investigate the temporal and spatial variations of columnar aerosol properties over this poorly explored region.

Within the analysed period the daily average values of $\delta_a(500 \text{ nm})$ over Alborán Island ranged from 0.03 to 0.54 with a mean and standard deviation of 0.17 ± 0.12 , indicating high aerosol load variation. The observed mean $\delta_a(500 \text{ nm})$ value over Alborán Island was significantly higher than reported for open oceanic areas not affected by long range aerosol transport (0.06-0.08). The $\alpha(440-870)$ values were lower than 1 for 70% of the measurement days, suggesting that coarse particles dominated the aerosol population over the Alborán Island for the majority of the measurement days.

High aerosol loads over Alborán were mainly associated with desert dust transport from arid areas in North Africa and occasional advection of anthropogenic fine particles from central European urban-industrial areas. The aerosol optical depth values of fine mode during dust events were also relatively high (for this remote site), suggesting that the fine mode particles also have considerable influence on optical properties during these dust events. Background maritime conditions over Alborán characterized by low aerosol load and Ångström exponent ($\delta_a(500 \text{ nm}) < 0.15$ and $\alpha(440-870) < 1$) were observed on about 40% of the measurement days during the analyzed period; almost all of these days were characterized by advection of clean Atlantic air masses over the study area.

The mean value of $\delta_F(500 \text{ nm})$ over Alborán Island was comparable to the observations over the other three nearby AERONET stations, suggesting homogeneous spatial distribution of fine particle loads over the four studied sites in spite of the large differences in local sources. A northward decreases in $\delta_C(\lambda)$ was found which was probably associated with increased desert dust deposition from south to north or decreased dust frequency from South to north.

Aerosol properties acquired on board the ship Nautilus_11 within Maritime Aerosol Network over the whole Mediterranean Sea, Black Sea and Atlantic Ocean from July to November 2011 showed large variability and no evident pattern was found. In 85% of the measurements, the fine mode fraction was in the range 0.52-0.96, indicating the predominance of fine mode particles over the cruise areas during the monitoring period.

1 The highest $\delta_a(500 \text{ nm})$ and $\delta_F(500 \text{ nm})$ mean values of 0.35 ± 0.09 and 0.29 ± 0.09 during
2 the cruise period were observed over the western Mediterranean Sea, which were
3 related to polluted air masses coming from European urban-industrial areas. In contrast,
4 the lowest $\delta_a(500 \text{ nm})$ values (mean value of 0.14 ± 0.06) during this cruise were
5 observed over the eastern Mediterranean Sea on the final days of the cruise in autumn,
6 when aerosol wet deposition is more effective and secondary aerosol formation is less
7 important than in summer.

8 **Acknowledgments**

9 This work was supported by the Andalusia Regional Government through projects P12-
10 RNM-2409 and P10-RNM-6299, by the Spanish Ministry of Science and Technology
11 through projects CGL2010-18782, and CGL2013-45410-R; and by the EU through
12 ACTRIS project (EU INFRA-2010-1.1.16-262254). CIMEL Calibration was performed
13 at the AERONET-EUROPE calibration center, supported by ACTRIS (European Union
14 Seventh Framework Program (FP7/2007-2013) under grant agreement no. 262254. The
15 authors gratefully acknowledge the outstanding support received from Royal Institute
16 and Observatory of the Spanish Navy (ROA). The authors are grateful to the
17 AERONET, MAN, and field campaign PIs for the production of the data used in this
18 research effort. We would like to express our gratitude to the NASA Goddard Space
19 Flight Center, NOAA Air Resources Laboratory and Naval Research Laboratory for the
20 HYSPLIT model. We would like to acknowledge the constructive comments of A.
21 Smirnov about the AERONET data. Finally, we also thank Dr Andrew Kowalski for
22 revising the manuscript.

23

1 **References**

- 2 Alados-Arboledas, L., Lyamani, H., and Olmo, F. J.: Aerosol size properties at Armilla,
3 Granada (Spain), *Q. J. R. Meteorol. Soc.*, 129, 1395–1413, 2003.
- 4 Alados-Arboledas, L., Muller, D., Guerrero-Rascado, J. L., Navas- Guzman, F., Perez-
5 Ramirez, D., and Olmo, F. J.: Optical and microphysical properties of fresh biomass
6 burning aerosol retrieved by Raman lidar, and star-and sun-photometry, *Geophys. Res.*
7 *Let.*, 38, L01807, doi:10.1029/2010gl045999, 2011.
- 8 Antón, M., Valenzuela, A., Cazorla, A., Gil, L. E., Fernandez-Galvez, J., Lyamani, H.,
9 Foyo-Moreno, I., Olmo, F. J., and Alados-Arboledas, L.: Global and diffuse shortwave
10 irradiance during a strong desert dust episode at Granada (Spain), *Atmos. Res.*, 118,
11 232-239, doi: I O. 10 16/j .atmosres.20.12. 07.007, 2012.
- 12 Balis, D., Amiridis, V., Zerefos, C., Gerasopoulos, E., Andreae, M. O., Zanis, P.,
13 Kazantzidis, A., Kazadzis, S., and Papayannis, A.: Raman lidar and Sunphotometric
14 measurements of aerosol optical properties over Thessaloniki, Greece during a biomass
15 burning episode, *Atmos. Environ.*, 37, 4529– 4538, 2003.
- 16 Barnaba, F. and Gobbi, G. P.: Aerosol seasonal variability over the Mediterranean
17 region and relative impact of maritime, continental and Saharan dust particles over the
18 basin from MODIS data in the year 2001, *Atmos. Chem. Phys.*, 4, 2367–2391,
19 doi:10.5194/acp-4-2367-2004, 2004.
- 20 Becagli, S., Sferlazzo, D. M., Pace, G., di Sarra, A., Bommarito, C., Calzolari, G.,
21 Ghedini, C., Lucarelli, F., Meloni, D., Monteleone, F., Severi, M., Traversi, R., and
22 Udisti, R.: Evidence for heavy fuel oil combustion aerosols from chemical analyses at
23 the island of Lampedusa: a possible large role of ships emissions in the Mediterranean,
24 *Atmos. Chem. Phys.*, 12, 3479–3492, doi:10.5194/acp-12-3479-2012, 2012.
- 25 Boselli, A., Caggiano, R., Cornacchia, C., Madonna, F., Mona, L., Macchiato, M.,
26 Pappalardo, G., and Trippetta, S.: Multi year Sun photometer measurements for aerosol
27 characterization in a Central Mediterranean site, *Atmos. Res.*, 104–105, 98–110,
28 doi:10.1016/ j.atmosres.2011.08.002, 2012.
- 29 Di Biagio, C., di Sarra, A., and Meloni, D.: Large atmospheric shortwave radiative
30 forcing by Mediterranean aerosols derived from simultaneous ground-based and
31 spaceborne observations and dependence on the aerosol type and single scattering
32 albedo, *J. Geophys. Res.*, 115, D10209, doi.org/10.1029/2009JD012697, 2010.

1 Di Iorio, T., Sarra, A. D., Junkermann, W., Cacciani, M., Fiocco, G., and Fuà, D.:
2 Tropospheric aerosols in the Mediterranean: 1. Microphysical and optical properties, *J.*
3 *Geophys. Res.*, 108(D10), 4316, doi:10.1029/2002JD002815, 2003.

4 Di Sarra, A., Pace, G., Meloni, D., De Silvestri, L., Piacentino, S., and Monteleone, F.:
5 Surface shortwave radiative forcing of different aerosol types in the central
6 Mediterranean, *Geophys. Res. Lett.*, 35, L02714. doi.org/10.1029/2007GL032395,
7 2008.

8 Draxler, R. R. and Rolph, G. D.: HYSPLIT (Hybrid Single-Particle Lagrangian
9 Integrated Trajectory). Model access via NOAA ARL READY website
10 <http://ready.arl.noaa.gov/HYSPLIT.php> (last access: May 2012), 2003.

11 Dubovik, O., Holben, B., Eck, T. F., Smirnov, A., Kaufman, Y. J., King, M. D., Tanre,
12 D., and Slutsker, I.: Variability of absorption and optical properties of key aerosol types
13 observed in worldwide locations, *J. Atmos. Sci.*, 59, 590–608, 2002.

14 Estellés, V., Martínez-Lozano, J. A., Utrillas, M. P., and Campanelli, M.: Columnar
15 aerosol properties in Valencia (Spain) by groundbased Sun photometry, *J. Geophys.*
16 *Res.-Atmos.*, 112, D11201, doi:10.1029/2006jd008167, 2007.

17 Estellés, V., Campanelli, M., Smyth, T. J., Utrillas, M. P., and Martínez-Lozano, J. A.:
18 Evaluation of the new ESR network software for the retrieval of direct sun products
19 from CIMEL CE318 and PREDE POM01 sun-sky radiometers. *Atmos. Chem. Phys.*,
20 12, 11619–11630, 2012.

21 Formenti, P., Andreae, M., Andreae, T., Galani, E., Vasaras, A., Zerefos, C., Amiridis,
22 V., Orlovsky, L., Karnieli, A., Wendisch, M., Wex, H., Holben, B., Maenhaut, W., and
23 Lelieveld, J.: Aerosol optical properties and large-scale transport of air masses:
24 observations at a coastal and a semiarid site in the eastern Mediterranean during
25 summer 1998, *J. Geophys. Res.*, 106, 9807–9826, doi:10.1029/2000JD900609, 2001.

26 Forster, P., Ramaswamy, V., Artaxo, P., Berntsen, T., Betts, R., Fahey, D. W.,
27 Haywood, J., Lean, J., Lowe, D. C., Myhre, G., Nganga, J., R. Prinn, Raga, G., Schulz,
28 M., and Dorland, R. V.: Changes in Atmospheric Constituents and in Radiative Forcing,
29 *Climate Change 2007: The Physical Science Basis*, Contribution of Working Group I to
30 the Fourth Assessment Report of the Intergovernmental Panel on Climate Change,
31 edited by: Solomon, S., Qin, D., Manning, M., Chen, Z., Marquis, M., Averyt, K. B.,
32 Tignor, M., and Miller, H. L., 2007.

1 Fotiadi, A., Hatzianastassiou, N., Drakakis, E., Matsoukas, C., Pavlakis, K.G.,
2 Hatzidimitriou, D., Gerasopoulos, E., Mihalopoulos, N., Vardavas, I.: Aerosol physical
3 and optical properties in the Eastern Mediterranean Basin, Crete, from Aerosol Robotic
4 Network data, *Atmos. Chem. Phys.*, 6, 5399–5413, 2006.

5 Foyo-Moreno I., Alados, I., Antón, M., Fernández-Gálvez, J., Cazorla, A., and Alados-
6 Arboledas, L.: Estimating aerosol characteristics from solar irradiance measurements at
7 an urban location in southeastern Spain. *J. Geophys. Res.*, 119, 1845–1859,
8 doi:10.1002/2013JD020599, 2014.

9 Gerasopoulos, E., Andreae, M. O., Zerefos, C. S., Andreae, T. W., Balis, D., Formenti,
10 P., Merlet, P., Amiridis, V., and Papastefanou, C.: Climatological aspects of aerosol
11 optical properties in Northern Greece, *Atmos. Chem. Phys.*, 3, 2025–2041, 2003.

12 Haywood, J. M. and Shine K. P.: Multi-spectral calculations of the direct radiative
13 forcing of tropospheric sulphate and soot aerosols using a column model, *Q. J. Roy.
14 Meteor. Soc.*, 123, 1907–1930, 1997.

15 Haywood, J. and Boucher, O.: Estimates of the direct and indirect radiative forcing due
16 to tropospheric aerosols: a review, *Rev. Geophys.*, 38, 513-543, 2000.

17 Holben, B. N., Eck, T. F., Slutsker, I., Tanre, D., Buis, J. P., Setzer, A., Vermote, E.,
18 Reagan, J. A., Kaufman, Y. J., Nakajima, T., Lavenu, F., Jankowiak, I., and Smirnov,
19 A.: AERONET – A federated instrument network and data archive for aerosol
20 characterization, *Remote Sens. Environ.*, 66, 1–16, 1998.

21 Horvath, H., Alados Arboledas, L., Olmo, F.J., Jovanovic, O., Gangl, M., Sanchez, C.,
22 Sauerzopf, H., and Seidl, S.: Optical characteristics of the aerosol in Spain and Austria
23 and its effect on radiative forcing, *J. Geophys. Res.* 107, 4386.
24 doi:10.1029/2001JD001472, 2002.

25 Kaufman, Y. J., Wald, A. E., Remer, L. A., Gao, B. C., Li, R. R., and Flynn, L.: The
26 MODIS 2.1- μ m channel – Correlation with visible reflectance for use in remote
27 sensing of aerosol, *IEEE T. Geosci. Remote. Sens.*, 35, 1286–1298, 1997.

28 Kaufman, Y. J., Koren, I., Remer, L. A., Rosenfeld, D., and Rudich, Y.: The effect of
29 smoke, dust, and pollution aerosol on shallow cloud development over the Atlantic
30 Ocean, *Proceedings of the National Academy of Sciences of the United States of
31 America.*, 102(32), 11207–11212, 2005.

1 Knobelspiesse, K. D., Pietras, C., Fargion, G. S., Wang, M. H., Frouin, R., Miller, M.
2 A., Subramaniam, S., and Balch, W. M. : Maritime aerosol optical thickness measured
3 by handheld sunphotometers, *Remote Sens. Environ.*, 93, 87–106, 2004.

4 Kubilay, N., Cokacar, T., and Oguz T.: Optical properties of mineral dust outbreaks
5 over the north-eastern Mediterranean, *J. Geophys. Res.*, 108(D21), 4666,
6 doi:10.1029/2003JD003798, 2003.

7 Lelieveld, J., Berresheim, H., Borrmann, S., Crutzen, P. J., Dentener, F. J., Fischer, H.,
8 de Gouw, J., Feichter, J., Flatau, P., Heland, J., Holzinger, R., Korrmann, R., Lawrence,
9 M., Levin, Z., Markowicz, K., Mihalopoulos, N., Minikin, A., Ramanathan, V., de Reus,
10 M., Roelofs, G.-J., Scheeren, H. A., Sciare, J., Schlager, H., Schultz, M., Siegmund, P.,
11 Steil, B., Stephanou, E., Stier, P., Traub, M., Williams, J., and Ziereis, H.: Global air
12 Pollution crossroads over the Mediterranean, *Science*, 298, 794–799, 2002.

13 Lyamani, H., Olmo, F. J., and Alados-Arboledas, L.: Saharan dust outbreak over
14 southeastern Spain as detected by sun photometer, *Atmos. Environ.*, 39, 7276–7284,
15 doi:10.1016/j.atmosenv.2005.09.011, 2005.

16 Lyamani, H., Olmo, F. J., Alcantara, A., and Alados-Arboledas, L.: Atmospheric
17 aerosols during the 2003 heat wave in southeastern Spain I: Spectral optical depth,
18 *Atmos. Environ.*, 40, 6453–6464, doi:10.1016/j.atmosenv.2006.04.048, 2006a.

19 Lyamani, H., Olmo, F. J., Alcantara, A., and Alados-Arboledas, L.: Atmospheric
20 aerosols during the 2003 heat wave in southeastern Spain II: Microphysical columnar
21 properties and radiative forcing, *Atmos. Environ.*, 40, 6465–6476,
22 doi:10.1016/j.atmosenv.2006.04.047, 2006b.

23 Mallet, M., Roger, J. C., Despiaud, S., Dubovik, O., and Putaud, J. P.: Microphysical and
24 optical properties of aerosol particles in urban zone during ESCOMPTE, *Atmos. Res.*,
25 69, 73–97, 2003.

26 Mallet, M., Dubovik, O., Nabat, P., Dulac, F., Kahn, R., Sciare, J., Paronis, D., and
27 Léon, J. F.: Absorption properties of Mediterranean aerosols obtained from multi-year
28 ground-based remote sensing observations, *Atmos. Chem. Phys.*, 13, 9195–9210, 2013.

29 Markowicz, K. M., Flatau, P. J., Ramana, M. V., and Crutzen, P. J.: Absorbing
30 mediterranean aerosols lead to a large reduction in the solar radiation at the surface,
31 *Geophys. Res. Lett.*, 29, 1968, doi:10.1029/2002GL015767, 2002.

- 1 Meloni, D., di Sarra, G., Biavati, G., DeLuisi, J. J., Monteleone, F., Pace, G.,
2 Piacentino, S., and Sferlazzo, D. M.: Seasonal behaviour of Saharan dust events at the
3 Mediterranean island of Lampedusa in the period 1999–2005, *Atmos. Environ.*, 41,
4 3041–3056, 2007.
- 5 Meloni, D., di Sarra, A., Monteleone, F., Pace, G., Piacentino, S., and Sferlazzo, D. M.:
6 Seasonal transport patterns of intense Saharan dust events at the Mediterranean island of
7 Lampedusa. *Atmos. Res.* 88, 134–148, 2008.
- 8 Millán M.M., Salvador, R., Mantilla, E., and Kallos, G.: Photooxidant dynamics in the
9 Mediterranean basin in summer: results from European research projects. *Geophys. Res.*
10 *Lett.*, 102, (D7), 8811–8823, 1997.
- 11 Moulin, C., Lambert, C. E., Dayan, U., Masson, V., Ramonet, M., Bousquet, P.,
12 Legrand, M., Balkanski, Y. J., Guelle, W., Marticorena, B., Bergametti, G., and Dulac,
13 F.: Satellite climatology of African dust transport in the Mediterranean atmosphere, *J.*
14 *Geophys. Res.*, 103, 13 137–13 144, 1998.
- 15 O’Neill, N. T., Eck, T. F., Smirnov, A., Holben, B. N., and Thulasiraman, S.: Spectral
16 discrimination of coarse and fine mode optical depth, *J. Geophys. Res.-Atmos.*, 108,
17 4559, doi:10.1029/2002jd002975, 2003.
- 18 Pace, G., Meloni, D., and di Sarra, A.: Forest fire aerosol over the Mediterranean basin
19 during summer 2003, *J. Geophys. Res.- Atmos.*, 110, D21202,
20 doi:10.1029/2005jd005986, 2005.
- 21 Pace, G., di Sarra, A., Meloni, D., Piacentino, S., and Chamard, P.: Aerosol optical
22 properties at Lampedusa (Central Mediter- ranean). 1. Influence of transport and
23 identification of different aerosol types, *Atmos. Chem. Phys.*, 6, 697–713,
24 doi:10.5194/acp-6-697-2006, 2006.
- 25 Pandolfi, M., Gonzalez-Castanedo, Y., Alastuey, A., de la Rosa, J. D., Mantilla, E.,
26 Sánchez de la Campa, A., Querol, X., Pey, J., Amato, F., and Moreno, T.: Source
27 apportionment of PM₁₀ and PM_{2.5} at multiple sites in the strait of Gibraltar by PMF:
28 impact of shipping emissions, *Environ Sci Pollut Res.*, 18, 260–269, doi
29 10.1007/s11356-010-0373-4, 2011.
- 30 Papadimas C. D., Hatzianastassiou, N., Mihalopoulos, N., Querol, X., and Vardavas, I.:
31 Spatial and temporal variability in aerosol properties over the Mediterranean basin

1 based on 6 yr (2000–2006) MODIS data, *J. Geophys. Res.*, 113, D11205,
2 doi:10.1029/2007JD009189, 2008.

3 Papadimas, C. D., Hatzianastassiou, N., Matsoukas, C., Kanakidou, M., Mihalopoulos,
4 N., and Vardavas, I.: The direct effect of aerosols on solar radiation over the broader
5 Mediterranean basin, *Atmos. Chem. Phys.*, 12, 7165–7185, doi:10.5194/acp-12-7165-
6 2012, 2012.

7 Pérez-Ramírez, D., Lyamani, H., Olmo, F. J., Whiteman, D. N., and Alados-Arboledas,
8 L.: Columnar aerosol properties from sun and-star photometry: statistical comparisons
9 and day-to-night dynamic, *Atmos. Chem. Phys.*, 12, 9719–9738, doi:10.5194/acp-12-
10 9719-2012, 2012.

11 Saha, A., Mallet, M., Roger, J. C., Dubuisson, P., Piazzola, J., and Despiaud, S.: One
12 year measurements of aerosol optical properties over an urban coastal site: Effect on
13 local direct radiative forcing, *Atmos. Res.*, 90, 195–202, 2008.

14 Sayer, A. M., Smirnov, A., Hsu, N. C., and Holben, B. N.: A pure marine aerosol
15 model, for use in remote sensing applications, *J. Geophys. Res.*, 117, D05213,
16 doi:10.1029/2011JD016689, 2012a.

17 Sayer, A. M., Smirnov, A., Hsu, N. C., Munchak, L. A., and Holben B. N.: Estimating
18 marine aerosol particle volume and number from Maritime Aerosol Network data,
19 *Atmos. Chem. Phys.*, 12, 8889–8909, 2012b.

20 Smirnov, A., Holben, B. N., Kaufman, Y. J., Dubovik, O., Eck, T. F., Slutsker, I.,
21 Pietras, C., and Halthore, R.: Optical properties of atmospheric aerosol in maritime
22 environments, *J. Atmos. Sci.*, 59, 501–523, 2002.

23 Smirnov, A., Holben, B. N., Dubovik, O., Frouin, R., Eck, T. F., and Slutsker I.:
24 Maritime component in aerosol optical models derived from Aerosol Robotic Network
25 data, *J. Geophys. Res.*, 108(D1), 4033, doi:10.1029/2002JD002701, 2003.

26 Smirnov, A., Holben, B. N., Slutsker, I., Giles, D. M., Mc-Clain, C. R., Eck, T. F.,
27 Sakerin, S. M., Macke, A., Croot, P., Zibordi, G., Quinn, P. K., Sciare, J., Kinne, S.,
28 Harvey, M., Smyth, T. J., Piketh, S., Zielinski, T., Proshuninsky, A., Goes, J. I., Nelson,
29 N. B., Larouche, P., Radionov, V. F., Goloub, P., Moorthy, K. K., Matarresse, R.,
30 Robertson, E. J., and Jourdin, F.: Maritime Aerosol Network as a component of Aerosol
31 Robotic Network, *J. Geophys. Res.*, 112, D06204, doi:10.1029/2008JD011257, 2009.

1 Smirnov, A., Holben, B. N., Giles, D. M., Slutsker, I., O'Neill, N. T., Eck, T. F., Macke,
2 A., Croot, P., Courcoux, Y., Sakerin, S. M., Smyth, T. J., Zielinski, T., Zibordi, G.,
3 Goes, J. I., Harvey, M. J., Quinn, P. K., Nelson, N. B., Radionov, V. F., Duarte, C. M.,
4 Losno, R., Sciare, J., Voss, K. J., Kinne, S., Nalli, N. R., Joseph, E., Krishna Moorthy,
5 K., Covert, D. S., Gulev, S. K., Milinevsky, G., Larouche, P., Belanger, S., Horne, E.,
6 Chin, M., Remer, L. A., Kahn, R. A., Reid, J. S., Schulz, M., Heald, C. L., Zhang, J.,
7 Lapina, K., Kleidman, R. G., Griesfeller, J., Gaitley, B. J., Tan, Q., and Diehl, T. L.:
8 Maritime aerosol network as a component of AERONET – first results and comparison
9 with global aerosol models and satellite retrievals, *Atmos. Meas. Tech.*, 4, 583–597,
10 doi:10.5194/amt-4-583-2011, 2011.

11 Sumner, G., Homar, V., and Ramis, C.: Precipitation seasonality in Eastern and
12 Southern coastal Spain, *Int J Climatol.*, 21, 219–247, 2001.

13 Valenzuela, A., Olmo, F. J., Lyamani, H., Ant'ón, M., Quirantes, A., and Alados-
14 Arboledas, L.: Classification of aerosol radiative properties during African desert dust
15 intrusions over southeastern Spain by sector origins and cluster analysis, *J. Geophys.*
16 *Res.- Atmos.*, 117, D06214, doi:10.1029/2011JD016885, 2012a.

17 Valenzuela, A., Olmo, F. J., Lyamani, H., Antón, M., Quirantes, A., and Alados-
18 Arboledas, L.: Aerosol radiative forcing during African desert dust events (2005–2010)
19 over Southeastern Spain, *Atmos. Chem. Phys.*, 12, 10331–10351, 2012b.

20 Viana, M., Amato, F., Alastuey, A., Querol, X., Moreno, T., Dos Santos, S. G., Hecce,
21 M. D., and Fernández-Patier, R.: Chemical tracers of particulate emissions from
22 commercial shipping, *Environ. Sci. Technol.*, 43, 19, 7472-7477, 2009.

23 Thieuleux, F., Moulin, C., Breon, F. M., Maignan, F., Poitou, J., and Tanre D.: Remote
24 sensing of aerosols over the oceans using MSG/SEVIRI imagery, *Ann Geophys.*
25 *European Geosciences Union (EGU).*, 23, 12, 3561-3568.

26 Toledano, C., Cachorro, V. E., Berjon, A., de Frutos, A. M., Sorribas, M., de la Morena,
27 B. A., and Goloub, P.: Aerosol optical depth and Ångström exponent climatology at El
28 Arenosillo AERONET site (Huelva, Spain), *Q. J. Roy. Meteorol. Soc.*, 133, 795–807,
29 doi:10.1002/qj.54, 2007b.

30

1 Table 1. Statistical summary of daily mean values of spectral aerosol optical depth at
 2 1020, 500 and 340 nm, Ångström exponent, $\alpha(440-870)$, fine and coarse mode aerosol
 3 optical depths at 500 nm, $\delta_F(500 \text{ nm})$ and $\delta_C(500 \text{ nm})$, and fine mode fraction, FMF,
 4 observed over Alborán Island in the western Mediterranean during 1 July 2011 - 23
 5 January 2012; SD is the standard deviation and COV is the coefficient of variation.

6
7

	Mean	SD	Minimum	Maximum	COV(%)
$\delta_a(1020 \text{ nm})$	0.11	0.10	0.01	0.46	91
$\delta_a(500 \text{ nm})$	0.17	0.12	0.03	0.54	70
$\delta_a(340 \text{ nm})$	0.25	0.15	0.05	0.65	60
$\alpha(440-870)$	0.8	0.4	0.2	1.7	50
$\delta_F(500 \text{ nm})$	0.08	0.05	0.01	0.30	63
$\delta_C(500 \text{ nm})$	0.10	0.09	0.01	0.4	90
FMF	0.47	0.15	0.20	0.94	32

8
9

1 Table 2. Average values and standard deviations of $\delta_a(\lambda)$, $\alpha(440-870)$, $\delta_F(500 \text{ nm})$ and
 2 FMF from 1 July 2011 to 23 January 2012 for Alborán Island, Málaga, Oujda and
 3 Palma de Mallorca. Only days with coincident measurements at Alborán and at each
 4 one of the additional AERONET stations are used for direct comparison.

	Alborán	Málaga	Alborán	Palma de Mallorca	Alborán	Oujda
$\delta_a(1020 \text{ nm})$	0.09±0.09	0.06±0.05	0.13±0.10	0.06±0.04	0.13±0.11	0.16±0.17
$\delta_a(870 \text{ nm})$	0.10±0.09	0.08±0.06	0.14±0.11	0.08±0.05	0.14±0.11	0.18±0.18
$\delta_a(670 \text{ nm})$	0.12±0.10	0.09±0.07	0.16±0.12	0.10±0.06	0.16±0.12	0.19±0.18
$\delta_a(500 \text{ nm})$	0.16±0.11	0.14±0.09	0.20±0.13	0.14±0.07	0.20±0.13	0.23±0.19
$\delta_a(440 \text{ nm})$	0.18±0.12	0.16±0.10	0.23±0.14	0.18±0.09	0.22±0.14	0.25±0.19
$\delta_a(380 \text{ nm})$	0.21±0.13	0.20±0.12	0.26±0.15	0.21±0.10	0.25±0.15	0.29±0.20
$\delta_a(340 \text{ nm})$	0.23±0.14	0.23±0.13	0.29±0.16	0.24±0.11	0.28±0.16	0.30±0.20
$\alpha(440-870)$	0.9±0.4	1.0±0.3	0.8±0.4	1.2±0.4	0.8±0.4	0.8±0.4
$\delta_F(500 \text{ nm})$	0.09±0.06	0.09±0.06	0.09±0.07	0.09±0.06	0.09±0.07	0.09±0.06
FMF	0.50±0.15	0.53±0.13	0.47±0.18	0.60±0.14	0.47±0.19	0.47±0.19
Number of coincident days	141	141	93	93	101	101

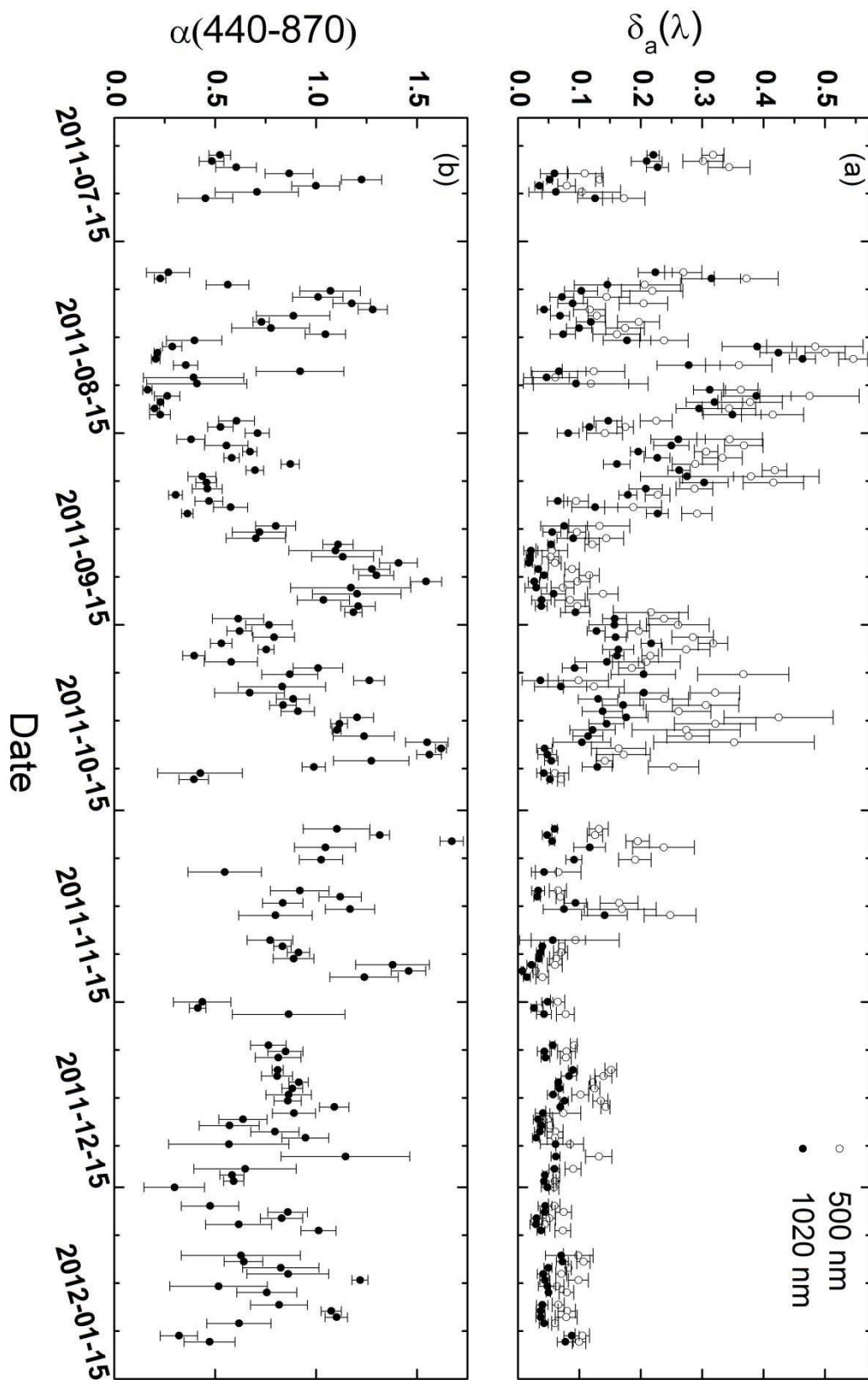
6
7

1 Table 3. Mean values of $\delta_a(500 \text{ nm})$, $\delta_F(500 \text{ nm})$, $\delta_C(500 \text{ nm})$, $\alpha(440-870)$ and FMF
 2 obtained over Black Sea, western, central and eastern Mediterranean Sea and Atlantic
 3 Ocean during the Nautilus ship cruise from 26 July to 13 November 2011.

4
5

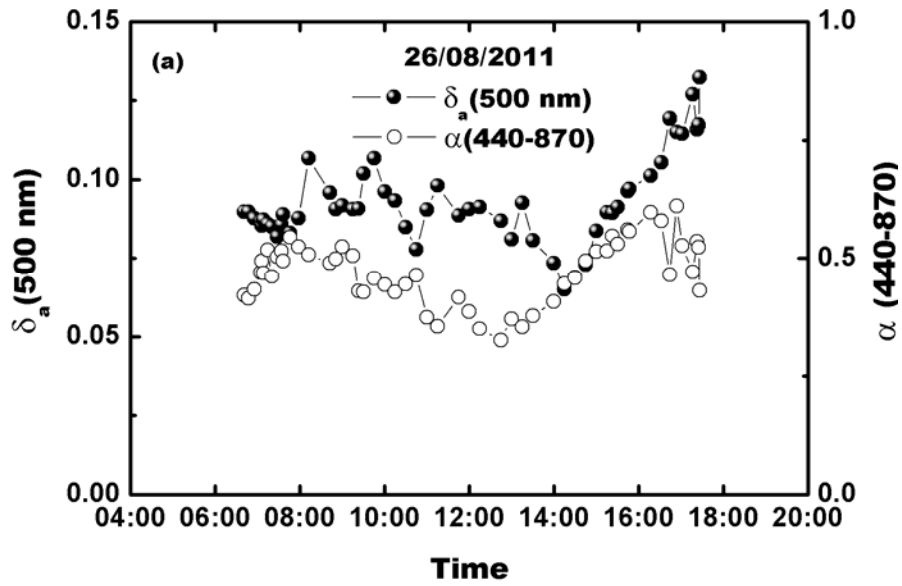
Region	$\delta_a(500 \text{ nm})$	$\delta_F(500 \text{ nm})$	$\delta_C(500 \text{ nm})$	$\alpha(440-870)$	FMF
Black Sea (26 July-15 August)	0.25±0.16	0.21±0.14	0.04±0.03	1.76±0.30	0.82±0.08
Eastern Mediterranean I (18 August-12 September)	0.20±0.08	0.16±0.07	0.04±0.02	1.74±0.20	0.81±0.08
Central Mediterranean I (13-28 September)	0.18±0.10	0.12±0.09	0.06±0.03	1.27±0.40	0.66±0.08
Western Mediterranean (28 September-8 October)	0.35±0.09	0.29±0.09	0.07±0.02	1.50±0.13	0.80±0.07
Atlantic Ocean (9-19 October)	0.19±0.10	0.11±0.05	0.09±0.06	1.08±0.25	0.56±0.09
Central Mediterranean II (25 October-5 November)	0.22±0.10	0.13±0.07	0.09±0.04	1.05±0.30	0.57±0.13
Eastern Mediterranean II (5-13 November)	0.14±0.06	0.07±0.02	0.08±0.04	0.90±0.35	0.49±0.12

6
7

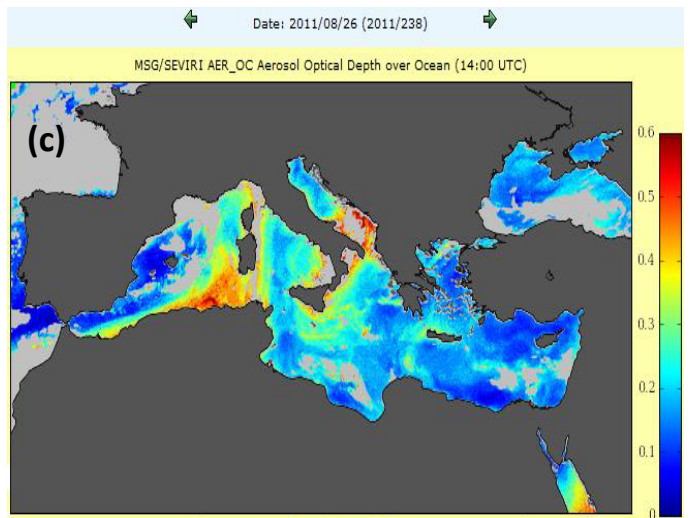
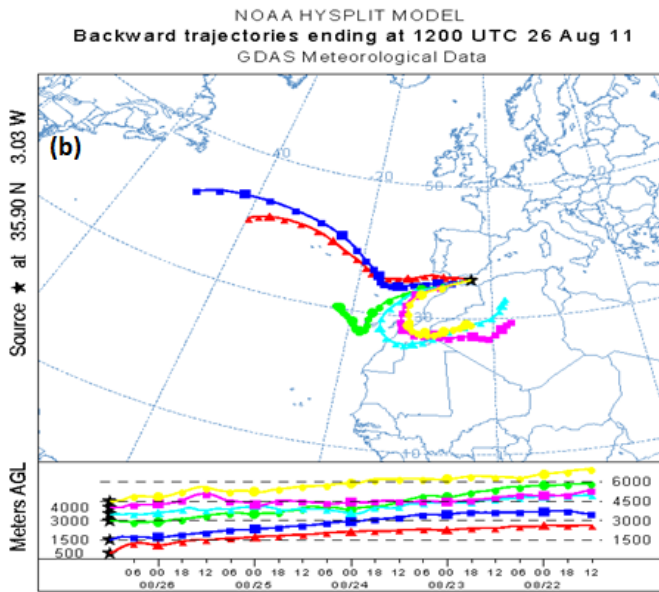


1 Figure 2. Temporal evolution of the daily mean values of (a) aerosol optical depth at
 2 500 and 1020 nm and (b) the Ångström exponent calculated in the range 440-870 nm,
 3 measured at Alborán Island in the western Mediterranean from 1 July 2011 to 23
 4 January 2012. The error bars are standard deviations.

5



8

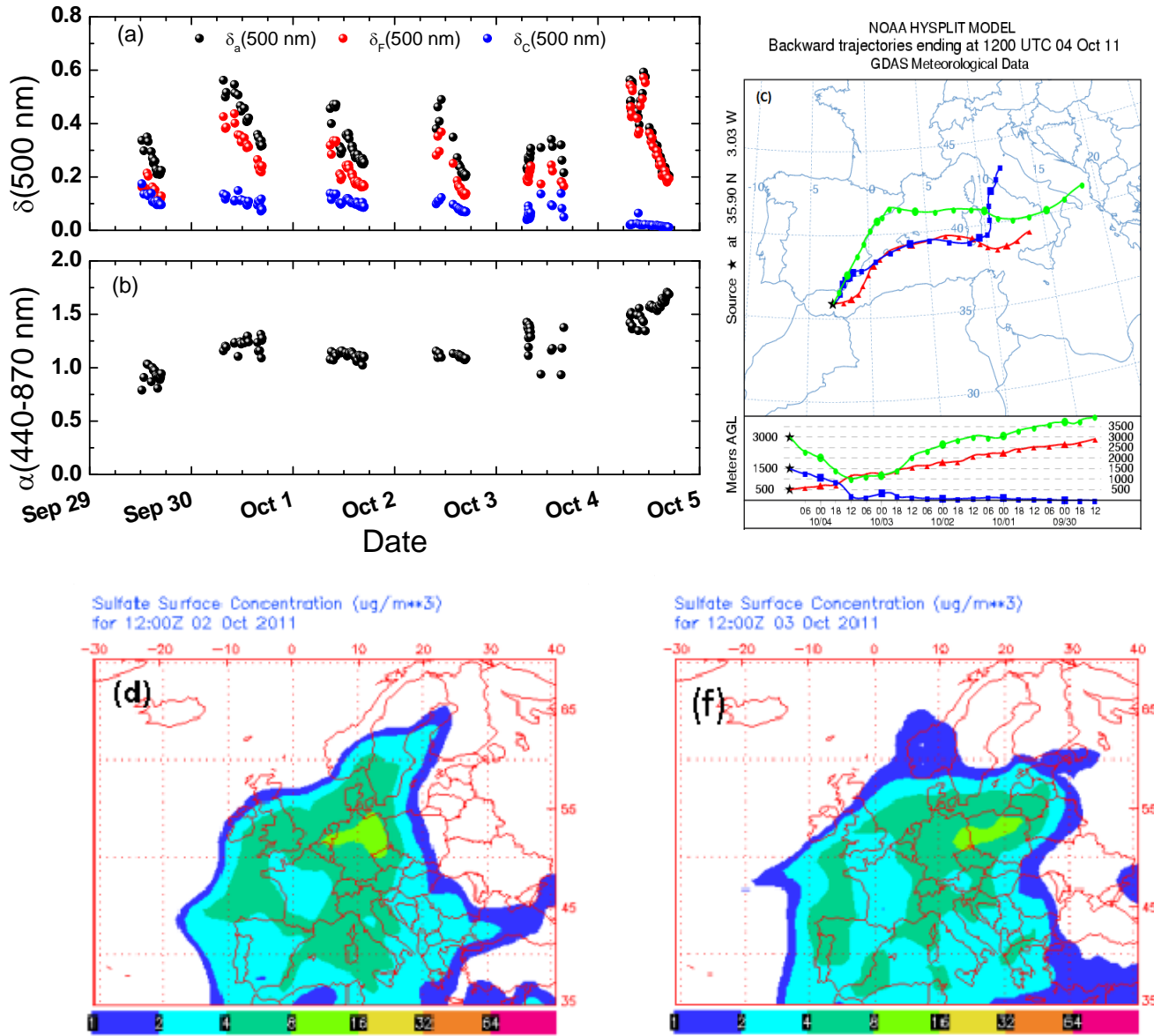


18

19 Figure 3. (a) Aerosol optical depth at 500 nm and Ångstrom exponent in the range 440-
 20 870 nm, (b) backward trajectories ending at 12 UTC over Alborán Island at height
 21 altitudes of 500, 1500, 3000 and 4000 m, (c) MSG satellite image for 26 August 2011
 22 (<http://www.icare.univ-lille1.fr>).

23

1
2



3

4 Figure 4. (a) Total, fine and coarse aerosol optical depths at 500 nm and (b) Ångström
 5 exponent in the range 440-870 nm obtained at Alborán Island during 29 September-5
 6 October 2011. (c) Backward trajectories ending at 12 UTC on 4 October 2011 over
 7 Alborán Island at altitudes of 500, 1500, 3000m. (d) and (f) NAAPS maps for sulfate
 8 surface concentrations for 2 and 3 October 2011 at 12:00 UTC

9

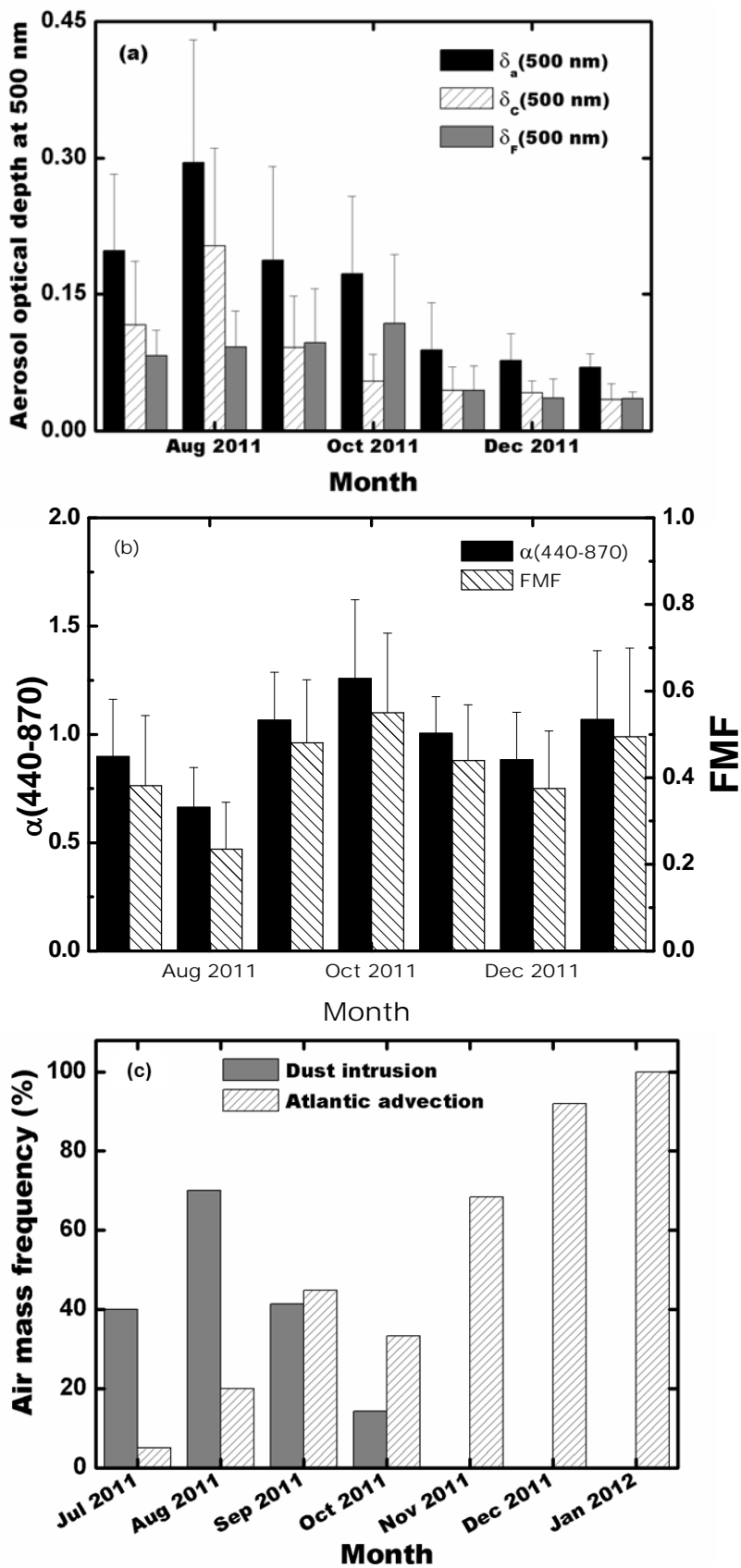
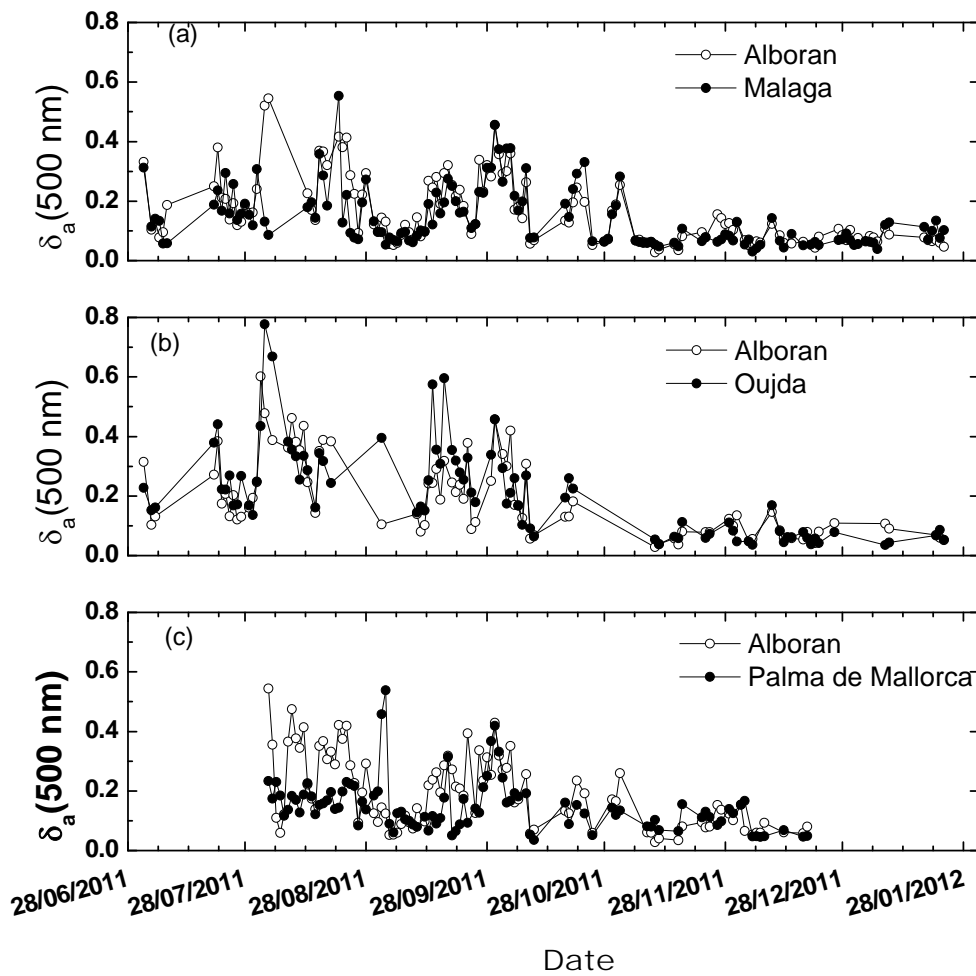
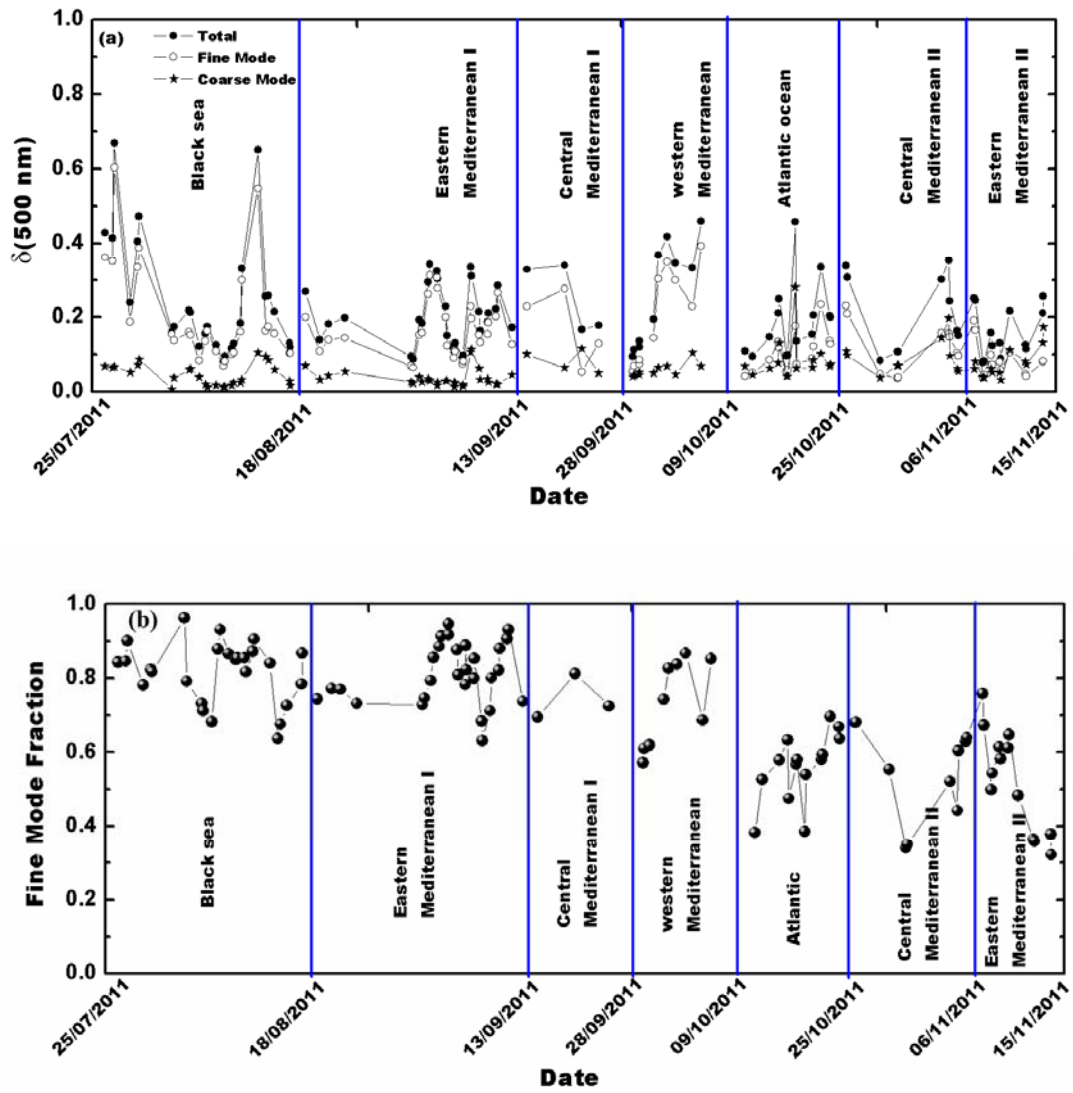


Figure 5. Monthly variations of (a) total, coarse and fine mode optical depths at 500 nm and (b) Fine mode fraction and Ångström exponent in the range 440-870 nm obtained at Alborán Island from July 2011 to January 2012. The error bars are standard deviations. (c) Monthly relative frequency of Saharan dust intrusions and Atlantic air mass advectations over Alborán Island from July 2011 to January 2012.



1 Figure 6. Temporal evolutions of daily mean values of $\delta_a(500 \text{ nm})$ from 1 July 2011 to
 2 23 January 2012 obtained over (a) Alborán Island and Málaga, (b) Alborán Island and
 3 Oujda and (c) Alborán Island and Palma de Mallorca. Daily mean data were calculated
 4 only from time coincident measurements.

5



1

2 Figure 7. Temporal evolutions of $\delta_a(500 \text{ nm})$, $\delta_F(500 \text{ nm})$, $\delta_C(500 \text{ nm})$, and FMF
 3 obtained on board of Nautilus ship. The data belong to the Maritime Aerosol Network
 4 (MAN) and were acquired between 26 July and 13 November 2011.
 5